Published on 04 March 2016. Downloaded by Ningbo Institute of Materials Technology and Engineering, CAS on 12/12/2016 00:42:07.

ChemComm

ROYAL SOCIETY OF CHEMISTRY

COMMUNICATION

View Article Online
View Journal | View Issue

Cite this: *Chem. Commun.*, 2016, **52**, 4828

Received 2nd February 2016,
Accepted 2nd March 2016

DOI: 10.1039/c6cc00989a

www.rsc.org/chemcomm

# Convertible resistive switching characteristics between memory switching and threshold switching in a single ferritin-based memristor†

Chaochao Zhang,‡[ab] Jie Shang,‡[b] Wuhong Xue,[b] Hongwei Tan,[b] Liang Pan,[b] Xi Yang,[b] Shanshan Guo,[b] Jian Hao,*[a] Gang Liu*[b] and Run-Wei Li*[b]

**A bio-memristor fabricated with ferritin exhibits novel resistive switching characteristics wherein memory switching and threshold switching are made steadily coexistent and inter-convertible through controlling the magnitude of compliance current presets.**

A memristive device based on resistive switching effect encodes '0' and '1' by switching between the low resistive state (LRS) and the high resistive state (HRS) under an external electric field.[1] Due to the simple structure, low power consumption, high operation speed and suitability for 3D ultrahigh density integration, the memristor has attracted a lot of attention for the potential applications of information storage, logic circuit and neuromorphic computing.[2,3] Commonly, resistive switching behaviour can be divided into two modes: non-volatile memory switching behaviour in which original LRS or HRS can be maintained even after the removal of the external electric field, and volatile threshold switching behaviour in which LRS is restored to HRS at a low bias voltage.[4] The former is often used as a memory device for information storage while the latter is chosen as a selector in series with a memory device to suppress the crosstalk problems in a cross-point or a multi-stack structure.[5] Moreover, volatile resistive switching also has great potential applications in the fields of neuromorphic computing and beyond von-Neumann computer architectures.[6] Over the past few years, some researchers have reported that the two types of resistive switching behaviours can coexist and inter-convert between each other in a single device with appropriate external stimulations.[7,8] Most of these functional layers are metal oxides that are fragile and poorly compatible with organisms, so they are hard to be applied in flexible and even implantable electronic devices.[9]

[a] Department of Chemistry, Shanghai University, Shanghai, 200444, P. R. China. E-mail: jhao@shu.edu.cn

[b] Key Laboratory of Magnetic Materials and Devices, Zhejiang Province Key Laboratory of Magnetic Materials and Application Technology, Ningbo Institute of Materials Technology and Engineering, Chinese Academy of Sciences, Ningbo, 315201, P. R. China. E-mail: liug@nimte.ac.cn, runweili@nimte.ac.cn

† Electronic supplementary information (ESI) available. See DOI: 10.1039/c6cc00989a

‡ These authors contributed equally to this work.

On the other hand, ferritin is a metalloprotein that can store and release iron to maintain a suitable level *in vivo* to sustain certain physiological functions.[10] It bears not only the basic characteristics of an organic material, such as light weight, easy fabrication process and mechanical flexibility,[11] but also the features of unique biodegradability, biocompatibility, non-toxicity and an abundant source that are good for economically viable, environmentally benign and implantable device applications.[12] In recent years, some efforts have been devoted to the investigation of the resistive switching characteristics of proteins.[12–14] Herein, we demonstrate that ferritin not only exhibits memory switching behaviour, but also shows threshold switching behaviour. Both behaviours can be inter-converted steadily.

Generally, ferritin has a nearly spherical shell and the iron ions are stored as the mineral core,[10] as schematized in Fig. 1a. Under the electric field, iron ions can be released from the shell, which is possibly responsible for the observed resistive switching effects.[10,13] In the present study, we have fabricated bio-memristor devices with the sandwich structure of the Pt/ferritin/Pt on a $SiO_2$/Si substrate. The surface topography and the thickness of the ferritin film were characterized by atomic force microscopy (AFM) and scanning electron microscopy (SEM),

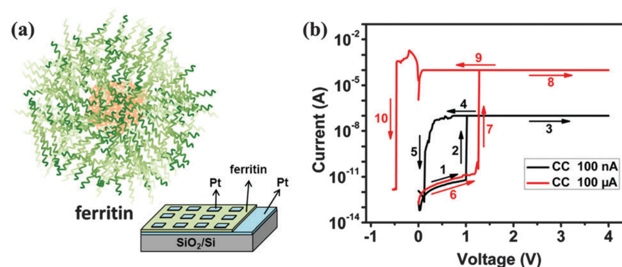


Fig. 1 (a) Schematic diagram of ferritin. The spherical shell consists of peptide subunits (green) and the mineral core consisting of hydrous iron oxide (orange). Lower right panel is the schematic illustration of the Pt/ferritin/Pt memristor on the $SiO_2$/Si substrate. (b) Non-volatile memory switching and volatile threshold switching of the Pt/ferritin/Pt device obtained with different current compliances.



This journal is © The Royal Society of Chemistry 2016

Published on 04 March 2016. Downloaded by Ningbo Institute of Materials Technology and Engineering, CAS on 12/12/2016 00:42:07.

respectively (Fig. S1 and S2, ESI†). The results show that the ferritin film has a promising morphological uniformity with a root-mean-square (rms) roughness of ∼3 nm and a thickness of ∼250 nm. In addition, X-ray photoelectron spectroscopy (XPS) indicates that the iron ion of the protein is trivalent (Fig. S3, ESI†).

To investigate the resistive switching behaviour of the Pt/ferritin/Pt device, the current–voltage ($I$–$V$) characteristics were measured using a Keithley 4200 semiconductor characterization system at room temperature. It is evident from Fig. 1b that both memory switching and threshold switching behaviours are achieved by adjusting the compliance currents (CCs). When the CC is 100 nA, we observe the threshold switching behaviour under DC voltage sweeps (0 V → 4 V → 0 V) at room temperature. Upon sweeping from 0 to 4 V, the current level abruptly increases at about 1.0 V and reaches the LRS; this is defined as the SET operation, and the voltage is defined as $V_{th}$. Then upon sweeping from 4 to 0 V, the current level abruptly decreases at about 0.15 V and the device is switched back to the HRS; this is defined as the RESET operation, and the voltage is defined as $V_{hold}$. Subsequently, we adjust the CC to 100 μA. The resistive switching behaviour is converted to memory switching. With the increase of the positive voltage, the device switches from the HRS to the LRS at about 1.3 V (this is also defined as the SET operation, wherein the voltage is defined as $V_{set}$) and the LRS can remain stable for a long time (>6 × 10$^3$ s, as shown in Fig. S4, ESI†) after the removal of the voltage. Then, upon sweeping the voltage reversely, the device switches back to the HRS at about −0.4 V (this is also defined as the RESET operation, wherein the voltage is defined as $V_{reset}$). This means that the $I$–$V$ characteristics exhibit a typical non-volatile bipolar switching behaviour. It is noteworthy that an unusual current increase can be observed in the negative sweep, wherein the CC of 100 μA has been employed in the respective positive scan to protect the device from current overshot and permanent breakdown. This can be ascribed to the discharging procedure of the parasitic capacitance of the semiconductor characterizing system and the ferritin device.[15]

Furthermore, we explore the electrical switching properties such as the resistance of HRS/LRS and switching voltages of $V_{set}$ and $V_{reset}$, as shown in Fig. 2. Fig. 2a displays the endurance characteristics of the non-volatile HRS and LRS for 70 switching cycles (read at 50 mV). Although the resistance in the ON state (LRS) and the OFF state (HRS) shows a slight fluctuation, the effective switching window is still clear in our device. The median resistance values of LRS and HRS are ∼510 Ω and ∼4 × 10$^8$ Ω, respectively. And the ON/OFF ratio is larger than 10$^5$ during the multiple consecutive voltage cycles (Fig. 2b). Further improvement of the device ON/OFF ratio can be made by inserting a metal oxide insulating layer between the electrode and the switching medium, which greatly suppresses the leakage current of the HRS.[16] Fig. 2c shows the cumulative distribution of SET and RESET voltages in the same 70 consecutive switching cycles. It is found that the SET and RESET voltages range from 0.5 V to 2.2 V and −0.16 V to −1.1 V respectively, and the SET voltage is generally larger than the RESET voltage.

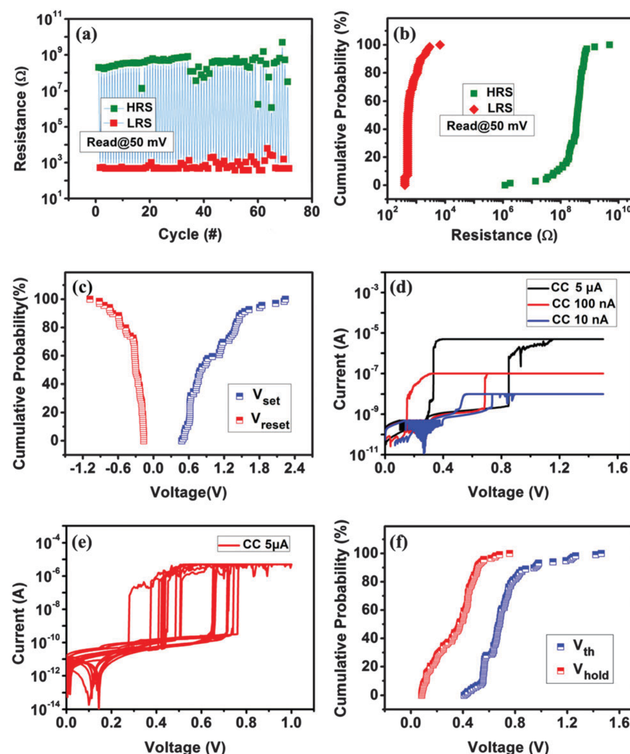


Fig. 2 (a) Endurance performance, (b) resistance and (c) switching voltage distributions of the non-volatile memory switching with a CC of 100 μA. (d) Typical $I$–$V$ curves with three different CCs of 5 μA, 100 nA and 10 nA. (e) Reproducibility and (f) switching voltage distribution of the volatile threshold switching.

It is worth noting that the volatile threshold switching can be held readily when the CC is less than 5 μA. And yet, threshold switching and memory switching are random when the CC is between 5 μA and 100 μA. Fig. 2d shows the $I$–$V$ curves with three different CCs of 5 μA, 100 nA and 10 nA. From this figure, we can see that they all show typical threshold switching behaviours. When sweeping the voltage reversely, a symmetric threshold switching loop can also be obtained, as shown in Fig. S5 (ESI†). Besides considering the CC, the impact of voltage is also studied. Fig. S6 (ESI†) shows the $I$–$V$ curves at different sweeping voltages of 1 V, 1.5 V, 2 V, 2.5 V and 3 V with the CC of 5 μA. It is found that the device can maintain the threshold switching behaviour at all sweeping voltages from 1 V to 3 V, implying that voltage has very little impact on the switching behaviour. The reproducibility of the threshold switching and the cumulative distribution of $V_{th}$ and $V_{hold}$ are also studied, as shown in Fig. 2e and f, which demonstrate minor fluctuation but are still applicable for selector applications.

More importantly, memory switching and threshold switching are made inter-convertible through controlling the magnitude of the CCs. First, the voltage-sweep mode is used for evaluation (Fig. 3a). It can be seen that the device can convert from threshold switching to memory switching repeatedly. Second, the pulse mode is used (Fig. 3b). When a stimulating pulse (amplitude of 1 V, width of 15 s) is applied, the response time of current is 0.7 s (with the CC of 100 μA) and 2.2 s (with the CC of 100 nA),

Published on 04 March 2016. Downloaded by Ningbo Institute of Materials Technology and Engineering, CAS on 12/12/2016 00:42:07.

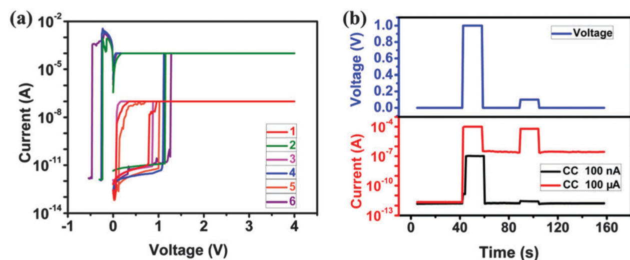


Fig. 3 (a) Transition between volatile and non-volatile switching with different CCs of 100 nA and 100 μA. (b) The responding current (black or red line) of a stimulating pulse (blue line) for the CCs of 100 nA and 100 μA.

respectively (Fig. S7, ESI†). The responding speeds, though relatively slower than that of the electronic devices, are nevertheless compatible with and suitable for physiological applications. Moreover, the current values (read at 0.1 V) have a great difference between two different CCs of 100 μA and 100 nA. When the CC is 100 μA, the current is about 60 μA which is slightly less compared to the CC (that is, the resistive switching is non-volatile); when the CC is 100 nA, the current is about 2.5 pA which is far less than the CC (that is, the resistive switching is volatile). These results further confirm that memory switching and threshold switching are made inter-convertible through controlling the magnitude of CC.

To understand the current transport mechanism inside the thin film, the non-volatile *I–V* curve is replotted in the log(*I*)–log(*V*) scale of Fig. S8 (ESI†). It is found that the conduction mechanism of the HRS at a low voltage is dominated by ohmic conduction (the slope of log(*I*)–log(*V*) curve is ~1). Upon the increase of applied voltage, the curve becomes slightly steeper and the slope is 1.7 (the linear relationship can be regarded as $I \propto V^2$), which indicates that the space-charge-limited-current (SCLC) conduction mode is activated.[17] When the applied voltage approaches the threshold, the HRS is converted to the LRS and the logarithmic plot of the *I–V* characteristics in the LRS is fitted with a straight line (slope = 1), indicating that the conductive current in the LRS also follows Ohm's law. The transport mechanism of the volatile switching behaviour is similar (Fig. S9, ESI†).

In order to probe the resistive switching mechanism in ferritin film, local electrical conduction is investigated by conductive atomic force microscopy (C-AFM) using the Pt–Ir cantilever tip as the top electrode (Fig. 4a). With the limited current compliance of the microscope (1.25 nA), the *I–V* curve demonstrates a volatile behaviour similar to that of the Pt/ferritin/Pt device (Fig. 4b). On the other hand, the current map of the pristine ferritin film has no apparent leakage at 50 mV (Fig. 4c), while multiple conductive spots arise when the applied voltage is increased to 1 V. This directly implies that the filamentary conduction mechanism is responsible for the resistive switching in ferritin devices (Fig. 4d). Considering the chemically inert nature of the platinum electrode, we propose that iron ions are the sources for constructing conductive filaments in ferritin films.[12] In the case of low CC preset (below 5 μA for the macroscopic device, for instance), the dimension and strength of the

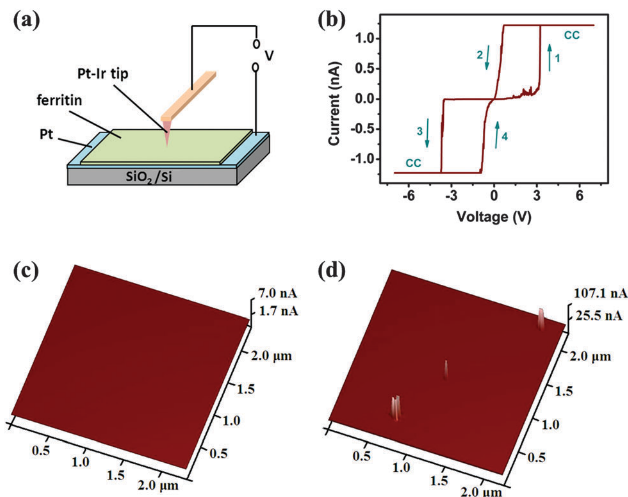


Fig. 4 (a) Simplified schematic diagram of the C-AFM measurement. (b) *I–V* characteristics of a single spot. (c) and (d) Current distribution upon being subjected to voltages of 50 mV and 1 V, respectively.

conductive filament would be really limited, which leads to the easily rupturing nature and thus volatile switching behaviour of the device.[3,7] When the CC preset is high enough (*e.g.* (100 μA)), memory switching can be expected with strong and stable conductive filaments. The schematic illustration of the mechanism is shown in Fig. S10 (ESI†).

In summary, a biocompatible memristor device based on natural ferritin has been fabricated. The device not only exhibits a non-volatile memory switching behaviour, but also shows a volatile threshold switching behaviour. More significantly, the two behaviours can be made reliably inter-convertible by controlling the magnitude of compliance current presets. The features mentioned above make it promising for novel logic and bioelectronic device applications.

This work was supported by the State Key Project of Fundamental Research of China (973 Program, 2012CB933004), the National Natural Science Foundation of China (51303194, 61328402, 61306152, 11474295, 61574146 and 51525103), the Instrument Developing Project of the Chinese Academy of Sciences (YZ201327), the Youth Innovation Promotion Association of the Chinese Academy of Sciences, Ningbo Major Project for Science and Technology (2014B11011), Ningbo Science and Technology Innovation Team (2015B11001), Ningbo Natural Science Foundation (2014A610152), and Ningbo International Cooperation Projects (2014D10005).

## Notes and references

1 X. J. Zhu, W. J. Su, Y. W. Liu, B. L. Hu, L. Pan, W. Lu, J. D. Zhang and R.-W. Li, *Adv. Mater.*, 2012, **24**, 3941; W. B. Zhang, C. Wang, G. Liu, J. Wang, Y. Chen and R.-W. Li, *Chem. Commun.*, 2014, **50**, 11496; S. B. Long, C. Cagli, D. Ielmini, M. Liu and J. Sune, *J. Appl. Phys.*, 2012, **111**, 074508.

2 J. J. Yang, D. B. Strukov and D. R. Stewart, *Nat. Nanotechnol.*, 2013, **8**, 13; R. Waser and M. Aono, *Nat. Mater.*, 2007, **6**, 833; C. Moreno, C. Munuera, S. Valencia, F. Kronast, X. Obradors and C. Ocal, *Nano Lett.*, 2010, **10**, 3828; T. Hasegawa, T. Ohno, K. Terabe, T. Tsuruoka, T. Nakayama, J. K. Gimzewski and M. Aono, *Adv. Mater.*, 2010, **22**, 1831.

 This journal is © The Royal Society of Chemistry 2016

View Article Online



Published on 04 March 2016. Downloaded by Ningbo Institute of Materials Technology and Engineering, CAS on 12/12/2016 00:42:07.


3 Y. C. Yang, P. Gao, S. Gaba, T. Chang, X. Q. Pan and W. Lu, *Nat. Commun.*, 2012, **3**, 732.

4 H. T. Sun, Q. Liu, C. F. Li, S. B. Long, H. B. Lv, C. Bi, Z. L. Huo, L. Li and M. Liu, *Adv. Funct. Mater.*, 2014, **24**, 5679; S. H. Chang, J. S. Lee, S. C. Chae, S. B. Lee, C. Liu, B. Kahng, D.-W. Kim and T. W. Noh, *Phys. Rev. Lett.*, 2009, **102**, 026801.

5 Y.-J. Baek, Q. L. Hu, J. W. Yoo, Y. J. Choi, C. J. Kang, H. H. Lee, S.-H. Min, H.-M. Kim, K.-B. Kim and T.-S. Yoon, *Nanoscale*, 2013, **5**, 772; I. Hwang, M.-J. Lee, G.-H. Buh, J. Bae, J. Choi, J.-S. Kim, S. Hong, Y. S. Kim, I.-S. Byun, S.-W. Lee, S.-E. Ahn, B. S. Kang, S.-O. Kang and B. H. Park, *Appl. Phys. Lett.*, 2010, **97**, 052106.

6 Y. T. Li, P. Yuan, L. P. Fu, R. R. Li, X. P. Gao and C. L. Tao, *Nanotechnology*, 2015, **26**, 391001; T. Hasegawa, K. Terabe, T. Tsuruoka and M. Aono, *Adv. Mater.*, 2012, **24**, 252.

7 X. N. Zhao, H. Y. Xu, Z. Q. Wang, L. Zhang, J. G. Ma and Y. C. Liu, *Carbon*, 2015, **91**, 38.

8 J. Qi, M. Olmedo, J.-G. Zheng and J. L. Liu, *Sci. Rep.*, 2013, **3**, 2405; H. Y. Peng, Y. F. Li, W. N. Lin, Y. Z. Wang, X. Y. Gao and T. Wu, *Sci. Rep.*, 2012, **2**, 442; M. Yang, D. H. Bao and S. W. Li, *J. Phys. D: Appl. Phys.*, 2013, **46**, 495111; X. Saura, E. Miranda, D. Jimenez, S. B. Long, M. Liu, J. M. Rafi, F. Campabadal and J. Sune, *Jpn. J. Appl. Phys.*, 2013, **52**, 04CD06; L. He, Z.-M. Liao, H.-C. Wu, X.-X. Tian, D.-S. Xu, G. L. W. Cross, G. S. Duesberg, I. V. Shvets and D.-P. Yu, *Nano Lett.*, 2011, **11**, 4601.

9 L. Pan, Z. H. Ji, X. H. Yi, X. J. Zhu, X. X. Chen, J. Shang, G. Liu and R.-W. Li, *Adv. Funct. Mater.*, 2015, **25**, 2677.

10 R. Casiday and R. Frey, *Iron in Biology: Study of the Iron Content in Ferritin, The Iron-Storage Protein*, Washington University: St. Louis, MO, 2000.

11 W. B. Zhang, C. Wang, G. Liu, X. J. Zhu, X. X. Chen, L. Pan, H. W. Tan, W. H. Xue, Z. H. Ji, J. Wang, Y. Chen and R.-W. Li, *Chem. Commun.*, 2014, **50**, 11856.

12 Y.-C. Chen, H.-C. Yu, C.-Y. Huang, W.-L. Chung, S.-L. Wu and Y. K. Su, *Sci. Rep.*, 2015, **5**, 10022.

13 M. K. Hota, M. K. Bera, B. Kundu, S. C. Kundu and C. K. Maiti, *Adv. Funct. Mater.*, 2012, **22**, 4493; F. B. Meng, L. Jiang, K. H. Zheng, C. F. Goh, S. Lim, H. H. Hng, J. Ma, F. Boey and X. D. Chen, *Small*, 2011, **7**, 3016.

14 F. B. Meng, B. Sana, Y. G. Li, Y. J. Liu, S. Lim and X. D. Chen, *Small*, 2014, **10**, 277; H. Wang, Y. M. Du, Y. T. Li, B. W. Zhu, W. R. Leow, Y. G. Li, J. S. Pan, T. Wu and X. D. Chen, *Adv. Funct. Mater.*, 2015, **25**, 3825; H. Wang, F. B. Meng, Y. R. Cai, L. Y. Zheng, Y. G. Li, Y. J. Liu, Y. Y. Jiang, X. T. Wang and X. D. Chen, *Adv. Mater.*, 2013, **25**, 5498; H. Wang, F. B. Meng, B. W. Zhu, W. R. Leow, Y. Q. Liu and X. D. Chen, *Adv. Mater.*, 2015, **27**, 7670.

15 K. Kinoshita, K. Tsunoda, Y. Sato, H. Noshiro, S. Yagaki, M. Aoki and Y. Sugiyama, *Appl. Phys. Lett.*, 2008, **93**, 033506.

16 B. Cho, S. Song, Y. Ji and T. Lee, *Appl. Phys. Lett.*, 2010, **97**, 063305; D. C. Kim, M. J. Lee, S. E. Ahn, S. Seo, J. C. Park, I. K. Yoo, I. G. Baek, H. J. Kim, E. K. Yim, J. E. Lee, S. O. Park, H. S. Kim, U.-I. Chung, J. T. Moon and B. I. Ryu, *Appl. Phys. Lett.*, 2006, **88**, 232106; F. Yang, M. Wei and H. Deng, *J. Appl. Phys.*, 2013, **114**, 134502.

17 J. Zhang, H. Yang, Q.-L. Zhang, S. R. Dong and J. K. Luo, *Appl. Phys. Lett.*, 2013, **102**, 012113; B. L. Hu, F. Zhuge, X. J. Zhu, S. S. Peng, X. X. Chen, L. Pan, Q. Yan and R.-W. Li, *J. Mater. Chem.*, 2012, **22**, 520.